Ultrafast real-time vibronic coupling of a breather soliton in *trans*-polyacetylene using a laser pulse with few cycles

Takahiro Teramoto,[1,2] Zhuan Wang,[1,2] Valerii M. Kobryanskii,[3] Takashi Taneichi,[1,2] and Takayoshi Kobayashi[1,2,4,5]
[1]*Department of Applied Physics and Chemistry and Institute for Laser Science, University of Electro-Communications, 1-5-1 Chofugaoka, Chofu, Tokyo 182-8585, Japan*
[2]*International Cooperative Research Project (ICORP), Japan Science and Technology Agency, 4-1-8 Honcho, Kawaguchi, Saitama 332-0012, Japan*
[3]*Institute of Chemical Physics, Russian Academy of Science, Kosygin Street 4, Moscow 117977, Russia*
[4]*Department of Electrophysics, National Chiao Tung University, Hsinchu 30010, Taiwan*
[5]*Institute of Laser Engineering, Osaka University, 2-6 Yamada-oka, Suita, Osaka 565-0871, Japan*
(Received 7 November 2008; published 12 January 2009)

Simultaneous modulations of both frequencies and amplitudes of C–C and C=C stretching vibration modes, due to dynamical coupling to a breather soliton, in *trans*-polyacetylene was successfully time resolved. The frequency shifts of both modes were in good agreement with a simulation based on the Su-Schrieffer-Heeger model. It was found that the intensities of transition dipoles changed due to the breather, whereas transition energies were dominantly modulated by C=C stretching mode as recent theoretical work predicted.

DOI: 10.1103/PhysRevB.79.033202 PACS number(s): 78.66.Qn, 05.45.Yv, 63.22.−m, 78.47.J−

π-conjugated polymers have been attracting much attention of many scientists as one of the most promising materials for optoelectronic devices because of high conductivity and light-emitting efficiency. The rational design of novel plastic materials with enhanced functionalities for such devices requires deep insight into their electronic structure, charge and energy transport, and photoexcitation dynamics.

Trans-polyacetylene (*t*-PA) is the simplest π-conjugated polymer in which a nonlinear excitation, the soliton, is photogenerated, owing to strong electron-phonon coupling with a doubly degenerate ground state.[1–12] The soliton dynamics after photoexcitation is well investigated both experimentally[1,2,6–8,12] and theoretically,[9–11] motivated by the fact that its high conductivity is based on the soliton dynamics in the polymer chain, which can originate either from self-localized nonlinear excitations in small amount or from charge doping in abundance.[5]

The soliton dynamics in *t*-PA has been successfully interpreted by the Su-Schrieffer-Heeger (SSH) model about three decades ago.[3] Then several attempts have been made to improve the model.[10,11] Recently, with the aid of progress in computational technology, quantum chemical approaches such as time-dependent Hartree-Fock calculations also have been implemented.[13,14] In any cases theoretical models have predicted that a breather soliton is created, owing to the excess energy of photoexcitation and modulates the frequencies of stretching modes of C–C and C=C bonds during the ultrashort relaxation process from a photogenerated electron-hole pair to an unbound charged soliton-antisoliton pair.[9–14]

In this Brief Report, we revealed the modulated wave-packet real-time dynamics due to the electron-phonon coupling of the breather soliton in *t*-PA by ultrafast multichannel pump-probe spectroscopy and compared with the theoretical predictions. The sample was fabricated by polymerizing acetylene on a new rhenium catalyst in a highly viscous solution of polyvinyl butyral.[2] Both pump and probe pulses were derived from a noncollinear optical parametric amplifier (NOPA) system developed in our group.[15,16] The pump source of this system is commercially supplied regenerative amplifier (Spectra-Physics, Spitfire), whose pulse duration, center wavelength, repetition rate, and average output power were 50 fs, 790 nm, 5 kHz, and 800 mW, respectively. The visible NOPA pulse with 6.2-fs duration covered the photon energy range of 1.69–2.37 eV, with constant spectral phase throughout the whole laser spectrum. Pump-probe signals were detected with a 128-channel lock-in amplifier. Real-time vibration spectra were measured at delay time between the pump (40 nJ) and probe pulses (2 nJ) from −100 to 1100 fs with a 1-fs step.

In the photoexcitation of *t*-PA in the visible region of the NOPA output, an interband intrachain dipole-allowed π-π^* transition can take place. The peak (1.95 eV) in the absorption spectrum corresponds to the ^1B_u state.[17] Figure 1 shows the two-dimensional display of absorbance change (ΔA) of *t*-PA traced from −100 to 1100 fs of the pump-probe delay time over the whole probe spectral range. The observed $\Delta A(\omega,t)$ were decomposed into difference spectra with a set of three corresponding decay time constants, τ_1, τ_2, and τ_3, by a global fitting method as given by the following equation:

$$\Delta A(\omega,t) = A_1(\omega)\exp(-t/\tau_1) + A_2(\omega)\exp(-t/\tau_2) + A_3(\omega)\exp(-t/\tau_3). \quad (1)$$

The decay times of the signal were determined by the singular value decomposition method to be $\tau_1 = 66 \pm 20$ fs, $\tau_2 = 565 \pm 50$ fs, and $\tau_3 \gg 2$ ps by fitting Eq. (1) to the absorption spectra over the whole probe photon energy region. The shortest time constant, τ_1, is the lifetime of the electron-hole pair, which is in good agreement with values found in the literature.[8,13,14] The medium length decay time τ_2 corresponds to the lifetime of a charged soliton-antisoliton pair to geminate recombination.[8] The absolute value of the longest time constant τ_3 cannot be determined, with only a lower limit being obtained. However, this time constant is considered to be associated with the thermalization of the system, which does not necessarily have to be described with a single exponential decay constant, but can have complicated decay dynamics including diffusion process. The dynamics then

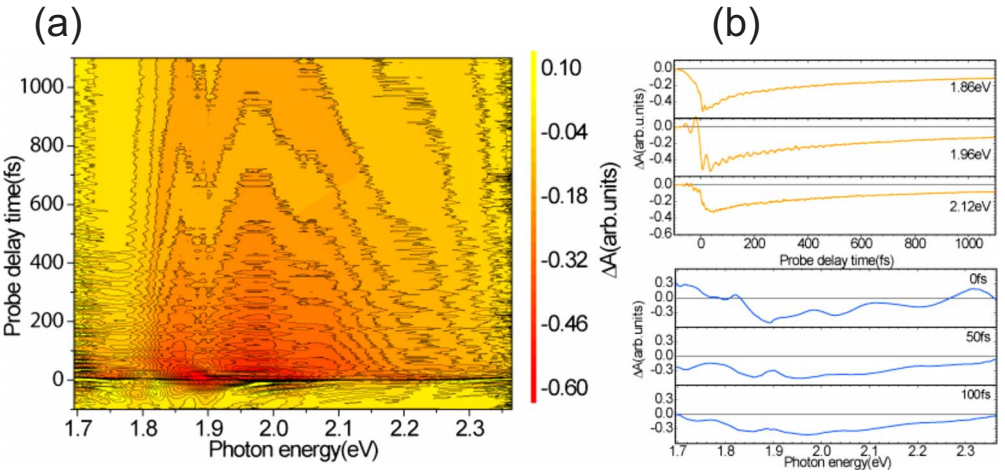

FIG. 1. (Color online) Two-dimensional real-time absorbance change spectrum of t-PA. (a) Two-dimensional display of $\Delta A(\omega,t)$ of t-PA. (b) The upper three show the real-time traces of ΔA at the photon energies of 1.86, 1.96, and 2.12 eV, respectively. The lower three show the photon energy dependencies of ΔA at the delay times of 30, 50, and 100 fs, respectively.

cannot be described by the rate equation, but by a diffusion equation considered to be taken place in the time range of 5–10 ps. It is well known that a signal in the "negative" delay-time range is due to perturbed free-induction decay.[18,19] Here the "negative" delay means that the probe pulse comes earlier than probe pulse to the sample position. From the probe-delay-time dependence of ΔA in the negative time range, the electronic dephasing time is determined to be 61 ± 14 fs, which is fairly close to the lifetime of the electron-hole pair (66 ± 20 fs). In a system with no pure dephasing or inhomogeneity the dephasing time is expected to be two times longer than the population decay time. Therefore the results indicate that a half of the fraction of electronic dephasing is induced by the population decay due to conversion of the electron-hole pair to an isolated charged soliton-antisoliton pair.

Probe-delay-time (t)-dependent change $[\delta\Delta A(\omega,t)]$ in $\Delta A(\omega,t)$ is due to the molecular vibration. Figure 2 shows the two-dimensional (ω,t) display of the fast Fourier transform (FFT) power spectra of real-time traces of $\Delta A(\omega,t)$ probed at the 128 photon energies in Fig. 1. The peak positions of the FFT amplitude due to C–C and C=C stretching modes were 1089 ± 6 and 1487 ± 10 cm^{-1}, respectively. The full width at half maximum (FWHM) of the peaks of each mode were 59 ± 2 and 70 ± 3 cm^{-1}, corresponding to the vibrational dephasing times of 570 ± 24 and 480 ± 14 fs, respectively. The dephasing times of both modes are close to the above-mentioned recombination time (565 ± 50 fs) of a charged soliton pair. This indicates that the dephasing of vibrational modes is determined partly by the recombination of the soliton pair and partly by the pure dephasing with nearly equal degree of contribution.

The result of spectrogram analysis[20–22] of the real-time trace at 1.71 eV is shown in Fig. 3. The probe-delay-time-dependent Fourier amplitude reveals the time evolution of C–C and C=C stretching modes with 1100 ± 8 and 1488 ± 8 cm^{-1}, respectively. In addition to the main skeleton oscillation, there exist four peaks at 305, 757, 1877, and 2254 with ambiguity of ± 8 cm^{-1}. The separation between the main bands and corresponding sidebands is 770 ± 40 cm^{-1} in all four cases. This frequency separation corresponds to a modulation period of 43 ± 3 fs, which is consistent with the breather period theoretically predicted (33–50 fs) (Refs. 9–11, 13, and 14) and the previously observed (44 ± 3 fs).[2] In the present work, these sidebands were observed in the whole photon energy range from 1.70 to 2.36 eV, which is considered to be the tail of the breather absorption with a peak located around 1.03 eV. The lifetime of the sideband amplitude in all cases is about 60 fs, which is in agreement with the electronic dephasing time of

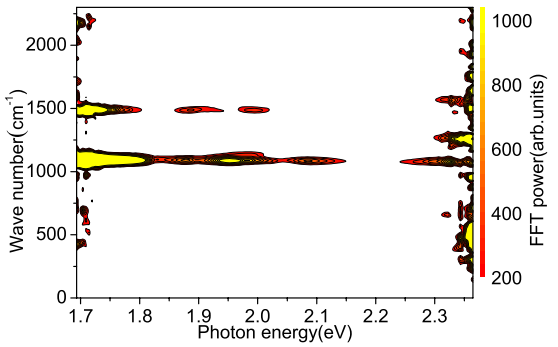

FIG. 2. (Color online) Two-dimensional display of FFT power spectra of t-PA.

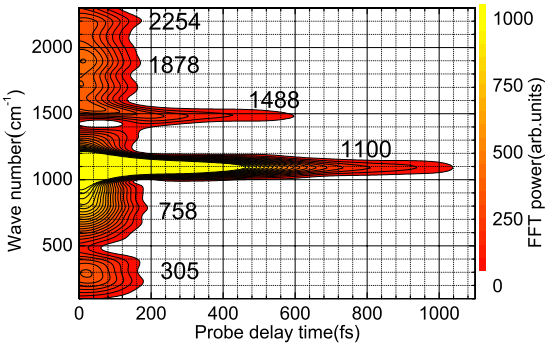

FIG. 3. (Color online) Two-dimensional display of spectrogram spectra of t-PA at 1.71 eV.

61 ± 14 fs within the experimental errors. The coincidence is explained in the following discussion.

The electronic coherence between an electron in the conduction band and a hole in the valence band is disturbed by the breather motion. The breather of the main chain strongly modulates the bond orders of both C–C single and double bonds within the extension of the soliton signal by driving π electrons from one C–C bond to the neighboring one. This is due to vibronic coupling and the electronic coherence is thus dissipated by the breather oscillation. The fast decay or disappearance[23] of the breather is also explained by dephasing and vibrational relaxation channels even on a single chain.[13,14] This is the observation of the transition state from the electron-hole pair with a breather to charged soliton pair with the localized breather at later delay time.

The modulation inducing the four sidebands to the C–C single and double bonds can be discussed in terms of amplitude and frequency modulations. The amplitude modulation (AM) on the vibrational amplitude $A(t)$ of C–C single and double bonds with vibrational frequency ω_0 can be described as follows:

$$\begin{aligned} A(t) &= A_0[1 + m_A(t)]\cos\,\omega_0 t \\ &= A_0\,\cos\,\omega_0 t + \frac{A_0 m_{A0}}{2}\cos(\omega_0 + \omega_m)t \\ &\quad + \frac{A_0 m_{A0}}{2}\cos(\omega_0 - \omega_m)t, \\ m_A(t) &= m_{A0}\,\cos\,\omega_m t. \end{aligned} \tag{2}$$

Here $m_A(t)$ is modulation function with amplitude m_{A0} and modulation frequency ω_m. In the case of frequency modulation (FM), the modulation due to the instantaneous frequency $m_F(t)$ is given by following equation written as Eq. (3):

$$\begin{aligned} A(t) &= A_0\,\cos\left(\omega_0 t + \int dt m_F\right) \\ &\approx A_0\,\cos\,\omega_0 t + \frac{A_0\phi_m}{2}\cos(\omega_0 + \omega_m)t \\ &\quad - \frac{A_0\phi_m}{2}\cos(\omega_0 - \omega_m)t, \\ m_F(t) &= \phi_m\omega_m\,\cos\,\omega_m t. \end{aligned} \tag{3}$$

In frequency modulation the amplitudes of sidebands show opposite phase unlike in the amplitude modulation. The ratio of amplitude fraction of FM to that of AM can be determined by $\phi_m/m_{A0}=(I_{\text{higher sideband}}-I_{\text{lower sideband}})/(1+I_{\text{higher sideband}})$. The ratio of FM to AM was determined as 0.11 for the C–C single stretching mode and 0.25 for the C=C double stretching mode. The frequency modulation is considered to be due to the modulation of the location of potential minimum along the corresponding vibrational coordinate maintaining its curvature in t-PA. On the other hand when the curvature of the harmonic potential is modulated, the amplitude of each mode is modulated, resulting in the periodical change in $\delta\Delta A$ on top of the electronic transition intensity, which is proportional to the Franck-Condon overlap between the initial and final states.

The profile of spectrogram from 0 to 80 fs with a 20 fs step is plotted in Fig. 4(a). The peak FFT amplitude of the C–C stretching mode shifts from 1155 to 1095 cm^{-1} with time evolution while that of the C=C stretching mode shifts from 1488.5 to 1503 cm^{-1}. Our scenario of the primary processes of photoexcitation follows the steps proposed in theoretical works.[24,25] The electron-hole pair formed by the photoexcitation associated with a localized breather mode relaxes to a separated pair of charged solitons with a localized breather mode. The observed frequency shifts are interpreted as a consequence of the coupling of the breather with the charged solitons. In the following, SSH Hamiltonian model[3,4] is calculated to describe above scenario. The model Hamiltonian is given as follows:

$$\begin{aligned} H = &-\sum_{n,s}[t_0 + \alpha(u_n - u_{n+1})][c^{\dagger}_{n+1,s}c_{n,s} + c^{\dagger}_{n,s}c_{n+1,s}] \\ &+ \frac{K}{2}\sum_n (u_n - u_{n+1})^2 + \frac{M}{2}\sum_n \dot{u}_n^2. \end{aligned} \tag{4}$$

u_n is the displacement of nth CH group in the polymer chain, t_0 is the π-band width, α is the electron-phonon coupling, K is the spring constant, and M is the mass of each CH group. $c^{\dagger}_{n,s}$ and $c_{n,s}$ are the creation and annihilation operators of π electron, respectively, with spin s for nth site. Based on the Hamiltonian, classical equations of motion for order parameters $\bar{\psi}_n(t) \equiv (-1)^n u_n/u_0$ and velocities $\dot{\bar{\psi}}_n$ are derived.[10] Here $u_0=0.04$ Å, assuming that the change in bond length due to dimerization from the nondimerized structure (that is, all bond orders are 1.5) is 0.08 Å.[9] Frequencies of the single and double bonds are determined experimentally to be 1095 and 1503 cm^{-1}, respectively. Calculated results and the observed data are shown in Fig. 4(a), revealing that the peak of the single bond redshifts while the peak of the double bond blueshifts. It is also shown that the initially localized excitation with a peak having an order parameter of −2 results in the two peaks being closer to each other. The time trace of bond order is estimated from both experimental and calculated data[26] [Fig. 4(b)]. The figure shows that the bond order of each bond exceeds 1 on the lower order side and is less than 2 on the higher side at the moment of electron-hole pair generation.

Recently, Tretiak *et al.*[13,14] found that the breather mode and C=C stretching mode mainly modulate the intensities (transition dipoles and oscillator strength) and transition energies, respectively. To verify these calculations, the zeroth and first derivatives of ΔA with respect to photon energy were compared with the probe photon energy dependence of FFT amplitude of spectrogram analysis [Figs. 4(c) and 4(d)]. The zeroth and first derivatives of ΔA correspond to the modulation of the transition intensity and that of the electronic transition energy, respectively. These results are consistent with the prediction made by Tretiak *et al.*[13,14]

In conclusion, it was directly verified that after photoexcitation, the electron-hole pair relaxes with a breather mode as theory[9–11,13,14] predicts with an electron-hole pair lifetime of 33–50 fs, which is in agreement with the electronic dephasing time. This is evidence of the correspondence between breather and electronic dephasing as predicted in the literature.[13,14] We could also determine the ultrafast phonon

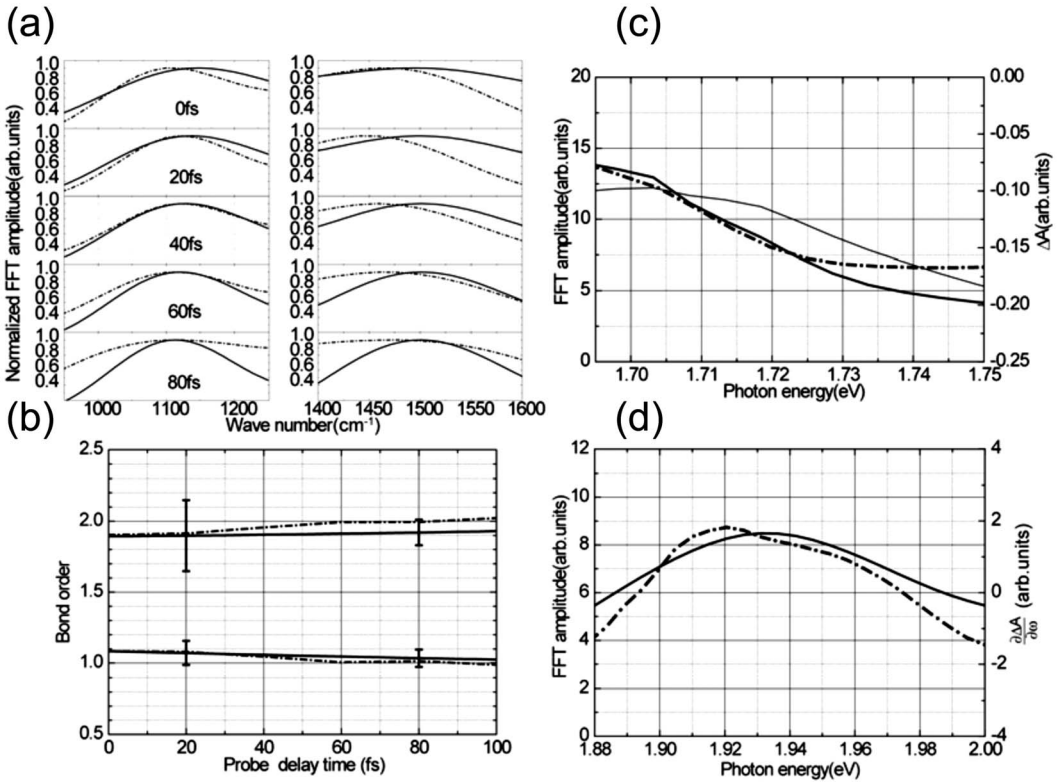

FIG. 4. Time traces and photon energy dependence of FFT amplitudes of C–C and C=C stretching and breather modes. (a) The results of experimental (solid line) and calculated (dot-dash-line) time traces of FFT amplitude of C–C and C=C stretching modes. (b) The time trace of bond order. (c) The probe photon energy dependence of FFT amplitude of sidebands of the C=C stretching mode (thin and thick solid lines correspond to the lower and higher sidebands, respectively) and zeroth derivative of $\Delta A(\omega,t)$ with respect to photon energy (dot-dashed line) at 50 fs. (d) The probe photon energy dependence of C=C stretching mode (solid line) and the first derivative of $\Delta A(\omega,t)$ with respect to photon energy (dot-dashed line) at 100 fs.

dynamics induced by the breather in *t*-PA: amplitude modulation, frequency modulation, and frequency shifts of C–C and C=C stretching modes. Calculation with the SSH Hamiltonian reproduced the time trace of the bond order of the C–C bonds in the polyacetylene. As theoretically predicted, it was found that the breather mode and the C=C stretching mode mainly modulate the transition intensity and transition energy, respectively.

The authors thank A. R. Bishop, S. Tretiak, and their group members for their fruitful comments. This work was partly supported by a grant from the Ministry of Education (MOE) in Taiwan under the ATU Program at National Chiao Tung University. A part of this work was performed under the joint research project of the Institute of Laser Engineering, Osaka University under Contract No. B1-27.

[1] G. S. Kanner *et al.*, Synth. Met. **116**, 71 (2001).
[2] S. Adachi *et al.*, Phys. Rev. Lett. **89**, 027401 (2002).
[3] W.-P. Su *et al.*, Phys. Rev. Lett. **42**, 1698 (1979).
[4] W.-P. Su *et al.*, Phys. Rev. B **22**, 2099 (1980).
[5] A. J. Heeger *et al.*, Rev. Mod. Phys. **60**, 781 (1988).
[6] M. Yoshizawa *et al.*, J. Phys. Soc. Jpn. **56**, 768 (1987).
[7] S. Takeuchi *et al.*, J. Chem. Phys. **105**, 2859 (1996).
[8] C. V. Shank *et al.*, Phys. Rev. Lett. **49**, 1660 (1982).
[9] W.-P. Su and J. R. Schrieffer, Proc. Natl. Acad. Sci. U.S.A. **77**, 5626 (1980).
[10] A. R. Bishop *et al.*, Synth. Met. **9**, 223 (1984).
[11] M. Sasai and H. Fukutome, Prog. Theor. Phys. **79**, 61 (1988).
[12] S. R. Phillpot *et al.*, Phys. Rev. B **40**, 1839 (1989).
[13] S. Tretiak *et al.*, Phys. Rev. B **70**, 233203 (2004).
[14] S. Tretiak *et al.*, Proc. Natl. Acad. Sci. U.S.A. **100**, 2185 (2003).
[15] A. Shirakawa *et al.*, Opt. Lett. **23**, 1292 (1998).
[16] A. Baltuska *et al.*, Opt. Lett. **27**, 306 (2002).
[17] L. Lüer *et al.*, Chem. Phys. Lett. **444**, 61 (2007).
[18] C. H. Brito Cruz *et al.*, IEEE J. Quantum Electron. **24**, 261 (1988).
[19] T. Kobayashi *et al.*, Phys. Rev. Lett. **101**, 037402 (2008).
[20] T. Kobayashi *et al.*, Nature (London) **414**, 531 (2001).
[21] T. Kobayashi *et al.*, Chem. Phys. Lett. **321**, 385 (2000).
[22] M. J. J. Vrakking *et al.*, Phys. Rev. A **54**, R37 (1996).
[23] G. Lanzani *et al.*, Phys. Rev. Lett. **90**, 047402 (2003).
[24] A. R. Bishop *et al.*, Phys. Rev. Lett. **52**, 671 (1984).
[25] S. Mukamel *et al.*, Science **277**, 781 (1997).
[26] R. H. Baughman *et al.*, J. Chem. Phys. **60**, 4755 (1974).